ELSEVIER

Journal of Electroanalytical Chemistry 453 (1998) 39–48

JOURNAL OF ELECTROANALYTICAL CHEMISTRY

Effects of mercury electrodeposition on the surface degradation of microlithographically fabricated iridium ultramicroelectrodes

Melissa A. Nolan, Samuel P. Kounaves *

Department of Chemistry, Tufts University, Medford, MA 02155, USA

Received 8 September 1997; received in revised form 20 April 1998

Abstract

The surface degradation of a microlithographically fabricated array of 10 μm diameter iridium ultramicroelectrodes (UME) was investigated using atomic force microscopy (AFM), Auger scanning electron microscopy (SEM), and stripping voltammetry. Micrometer-size accumulations could be observed on the iridium surface after mercury was electrochemically deposited and stripped approximately five times in a perchloric acid media with a Ag | AgCl | 3M NaCl reference electrode. AFM images of the accumulations revealed that they were pyramidal in shape and had a tendency to form in clusters. Elemental analysis of the clusters with Auger SEM identified them as mercury and a small amount of chloride. The accumulations were determined to be mercurous chloride (Hg_2Cl_2) with the chloride contamination resulting both from leakage of the reference electrode and the decay of the perchloric acid. During subsequent depositions of mercury, chloride ions were eliminated by using a nitric acid media and a polyurethane solid state reference electrode. With chloride eliminated, mercury could be electrodeposited and stripped at least ten times on the iridium UME array without any visible surface degradation.

Keywords: Iridium ultramicroelectrode array; Surface degradation; Mercury

1. Introduction

Over the past 10 years, ultramicroelectrode arrays have been widely employed for bioanalytical [1–5] and environmental [6–13] analysis with a major focus on heavy metal detection. One of the more commonly used techniques for fabrication, microlithography, creates well-defined and reproducible geometries of micron dimensions. In addition, several different types of materials can be utilized for the ultramicroelectrode array such as Au, Pt, Ag, Ir and various types of carbon.

The initial surface morphology and the ability to generate a well defined ultramicroelectrode (UME) surface are very important parameters in being able to obtain analytically reproducible data from such sensors. The topography of microlithographically fabricated UMEs can be studied using an atomic force microscope (AFM) [14]. Although scanning tunneling microscopy (STM) is more frequently utilized in studying electrode surfaces, difficulties arise when analyzing arrays because of the small ratio of conducting to insulating areas. This problem is overcome by the use of AFM since it can analyze both insulating and conducting surfaces. Ex-situ AFM was performed because the design and size of the array did not permit in-situ examination.

In electroanalysis, mercury still remains the electrode of choice for heavy metal detection when using such preconcentration techniques as anodic stripping voltammetry (ASV). The electrode substrate that the mercury is deposited onto is crucial because a 'true mercury' surface is preferred. UMEs made from Ag, Pt, or Au, are not suitable for formation of long-term mercury films because of their dissolution by the mercury film and the resulting formation of intermetallic compounds with the metals being analyzed. It has been

* Corresponding autho

0022-0728/98/$19.00
PII S0022-0728(98)00191-0

demonstrated that iridium is an excellent substrate for the formation of a mercury UME [15–17] because of its good wettability and low solubility (below 10^{-6} wt.%) in mercury [18,19]. The fabrication and characterization of mercury-plated iridium-based UME arrays has been well established [6–10,20].

During routine experiments with mercury coated iridium UME arrays (Ir-UMEAs) [20], the authors noted accumulations on the Ir UME array elements which could not be electrochemically removed. The current study utilizes AFM to determine the morphology and onset of these accumulations and Auger scanning electron microscopy (SEM) for their elemental analysis. In addition to assessing their nature, other aims of this work were to determine the possible sources of these accumulations and the observed surface degradation, and to develop methods for eliminating them in order to increase the lifetime of the UME arrays.

2. Experimental

2.1. Electrochemical apparatus

Controlled potential coulometry and linear sweep voltammetry experiments were performed using an EG&G PAR Model 273 potentiostat/galvanostat (EG&G PAR, Princeton, NJ) interfaced to a DEC p420-SX microcomputer and using the Model 270 software (EG&G PAR) for control. All voltammetric experiments were performed in a three electrode cell consisting of an Ir-UMEA, a Pt wire counter electrode and a Ag | AgCl | 3 M NaCl or a polyurethane solid state reference electrode (PU-SSRE) [21]. All potentials are reported relative to a Ag | AgCl | 3 M NaCl reference electrode.

2.2. Surface apparatus

Optical observations of the Ir-UMEAs were made with a Metaval-H (Leco/Jena) inverted microscope equipped with a video processing system. AFM images were obtained using a Digital Instruments Nanoscope E controller (Digital Instruments, Santa Barbara, CA). A custom made holder was used to support the circuit board during the imaging process. Auger SEM was performed with a Perkin Elmer/Physical Electronics Model 660 scanning Auger microprobe.

2.3. Microlithographic fabrication of iridium ultramicroelectrode arrays

The Ir-UMEAs were fabricated on a standard 10 cm wafer substrate. The wafer was cleaned and a 5000 Å layer of silicon dioxide was thermally grown on the surface. After coating with photoresist and patterning, an adhesive layer of titanium (300 Å) and the iridium layer (1000 Å) were deposited on the wafer by electron beam evaporation. A second photoresist and patterning was then used for the interconnect layer between the array elements and the bond pads. The interconnect metal, aluminum, was then evaporated by an electron beam. Since iridium cannot be chemically or plasma etched because of its inertness, a lift-off process was used to form the desired iridium pattern. To protect and insulate the conductors, a layer of silicon nitride (Si_3N_4) was deposited by low-temperature plasma enhanced chemical vapor deposition (PECVD). The silicon nitride was then selectively plasma etched to provide the active electrode configuration as shown in Fig. 1. The individual arrays were then diced into 5×16 mm chips and glued to a custom designed printed circuit (PC) board (CFC, Waltham, MA) with epoxy (Epo-Tek 905, Epoxy Technology, Billerica, MA). A connection between the bonding pad on the array and the PC board was formed with 1.25 μm Au wire (99.99%, Williams Advanced Materials, Buffalo, NY). The wire was then protected by a glob type epoxy (87-GT, Epoxy Technology Inc.) which was cured at 70°C for 3 h. The epoxy was kept out of the solution during the experiments in order to prevent any contamination.

2.4. Deposition of mercury

The Ir-UMEAs were initially cleaned in a mixture of sulfuric acid and hydrogen peroxide (30%) to remove any residual photoresist and then thoroughly rinsed with 18 MΩ cm deionized water. Mercury was deposited using controlled potential coulometry by applying a potential of -0.4 V until a total charge of approx. 480 μC was passed (charge being a better indicator of the amount of mercury being deposited).

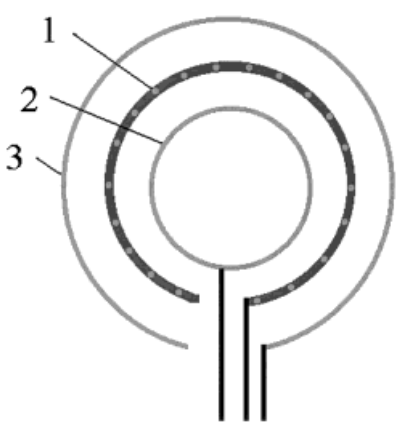

Fig. 1. Schematic of the Ir-UMEA which consisted of three concentric rings. The middle ring contains 20 disk iridium ultramicroelectrodes (1), each measuring 10 μm in diameter. The other two rings can be used as on-chip reference (2) or counter (3) electrodes.

The plating solutions consisted of 8×10^{-3} M Hg(II) in 0.1 M $HClO_4$ or 0.1 M HNO_3. Depositions of mercury on the Ir-UMEAs were confirmed by optical microscopy.

2.5. Stripping of mercury

Mercury was stripped using linear sweep voltammetry at a scan rate of 20 mV s^{-1} from -0.3 to 0.3 V in 1 M KSCN. The surface condition of the Ir-UMEAs was optically inspected before and after the stripping of mercury. AFM images were obtained immediately after the stripping of the mercury in order to determine the onset of the accumulations. The UME arrays were stored in a desiccator while not in use.

2.6. Reagents

All solutions were prepared with 18 MΩ cm deionized water from a Barnstead Nanopure system (Barnstead, Dubuque, IA). All glassware was stored in 8 M HNO_3 for a week and rinsed thoroughly with 18 MΩ cm deionized water. Mercury solutions were made with 99.999 + % $Hg(NO_3)_2$ (Johnson Matthey). Nitric and perchloric acid (Fisher) were trace metal grade. All other solutions were prepared with ACS grade reagents.

3. Results and discussion

3.1. Topography of iridium ultramicroelectrode surfaces

Two methods have been commonly used for microlithograhic deposition of iridium onto a silicon substrate, electron beam evaporation [9,20] or dc magnetron sputtering [6,7]. AFM images for both methods of deposition of iridium are shown in Fig. 2. Although the topography of the iridium surface was very different, good regularity and reproducibility were obtained over all the UMEs. The mean roughness of the iridium surface deposited by electron beam was 0.020 nm with a maximum height of 0.727 ± 0.30 nm. For the sputtered iridium surface, the mean roughness of 0.055 nm and the maximum height of 1.230 ± 0.35 nm was measured. The mean roughness was consistent for both surfaces, but the maximum height varied depending on the section of the UME analyzed. This difference in topography did not effect the electrodeposition of mercury, therefore, only electron beam evaporated iridium UME arrays were investigated.

3.2. Electrodeposition of Hg in perchloric acid and using a Ag | AgCl reference electrode

Mercury was electrodeposited and stripped from the Ir-UMEA five times. The AFM images showed no surface accumulations for the first three depositions of mercury. After the fourth deposition and stripping cycle, accumulations were observed on the iridium UMEs by optical microscopy and AFM. With the fifth coating of mercury, the amount of accumulations increased. Typical AFM images of the accumulations are shown in Fig. 3. The mean roughness of the iridium surface increased to 0.124 nm. The accumulations appeared pyramidal in shape (Fig. 3A) and were ~1.80 μm in width, 1.49 μm in length and 2.2 μm in height. Most of the accumulations seemed to cluster together as shown in Fig. 3B. The maximum height of the cluster was 4.16 μm and the width and length were 2.78 and 3.64 μm,

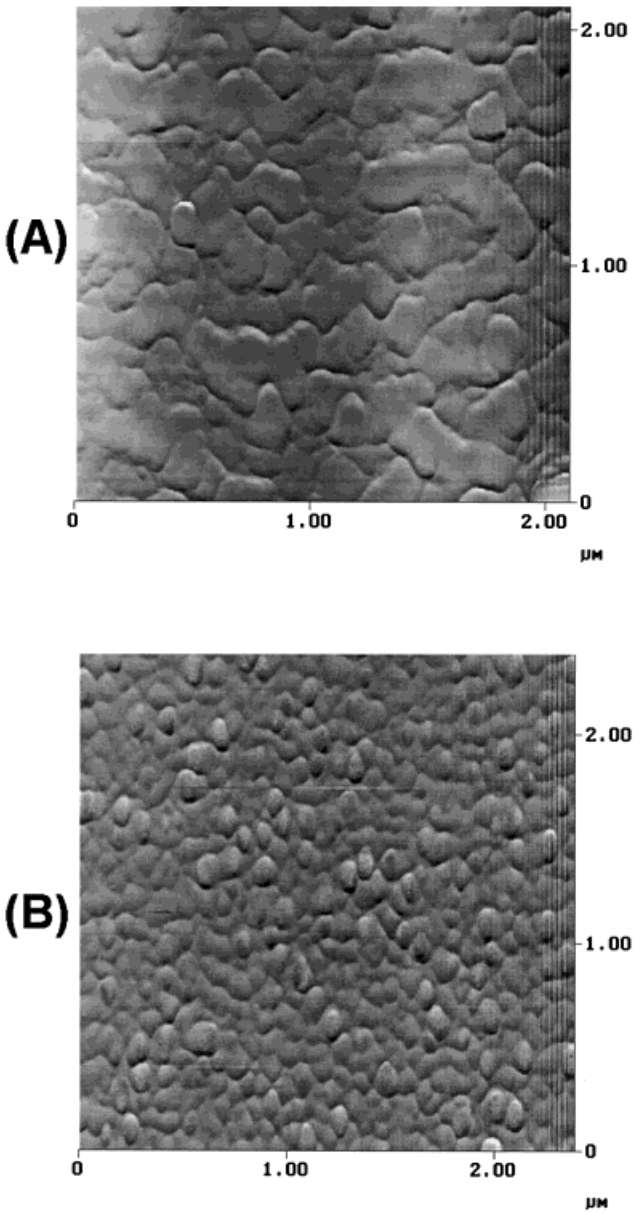

Fig. 2. AFM images of the iridium UME surfaces prior to Hg deposition for microfabrication via (A) dc magnetron sputtering and (B) electron beam evaporation.

respectively. Several individual pyramids were observed in the cluster. The congregation of the pyramids would not appear to be a coincidence since most of the accumulations on the electrode were clustered together.

3.2.1. Auger SEM analysis

For elemental analysis of the accumulations, Auger SEM was performed on the array. Spheres of mercury, in the range of 1–5 μm, were observed on the iridium surface indicating that some liquid mercury remained after the stripping process. During the analysis, the spheres were vaporized by the electron beam which left a rough iridium surface. Carbon and sulfur were found to be common contaminates during the Auger analysis but could be removed with argon sputtering.

The charging of the silicon nitride was an obstacle in performing Auger analysis on the Ir-UMEAs. The sides of the chip were coated with silver paint to minimize the charge build up but this was proven to be ineffective. Charge build up occurred especially on the edges of the UMEs and in several areas the iridium appeared to have 'burst'. A more descriptive image was obtained with the AFM (Fig. 4). The white area in the image is the iridium, which 'burst' and accumulated on the surface. The area to the right of this build up was a layer underneath the iridium of either titanium or silicon dioxide depending on the depth of the hole. The charge build up could be due to several reasons: (i) more conducting area was needed, (ii) there was a space between the iridium and its underlayers creating a 'hot spot' which burst or (iii) the beam voltage and other parameters needed to be adjusted to conform to the array. Although charging effects were still observed, the problem was minimized by using a greater amount of silver paint and applying it over a larger area of the array.

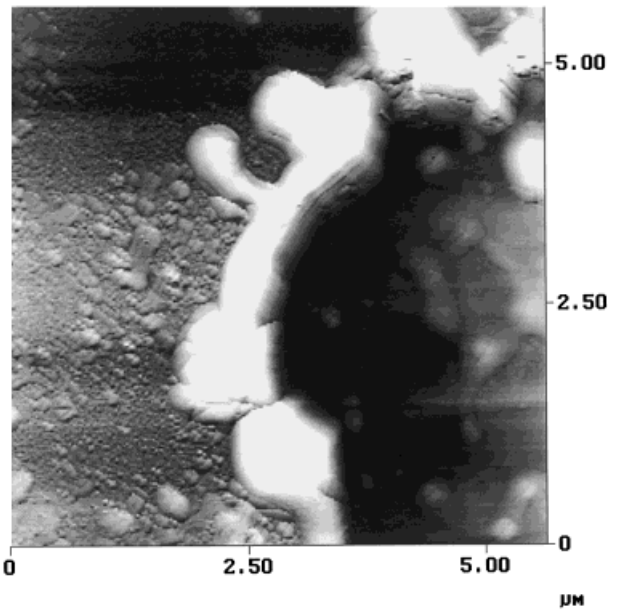

Fig. 4. AFM image of an Ir-UME that burst due to charge build up from the Auger electron beam.

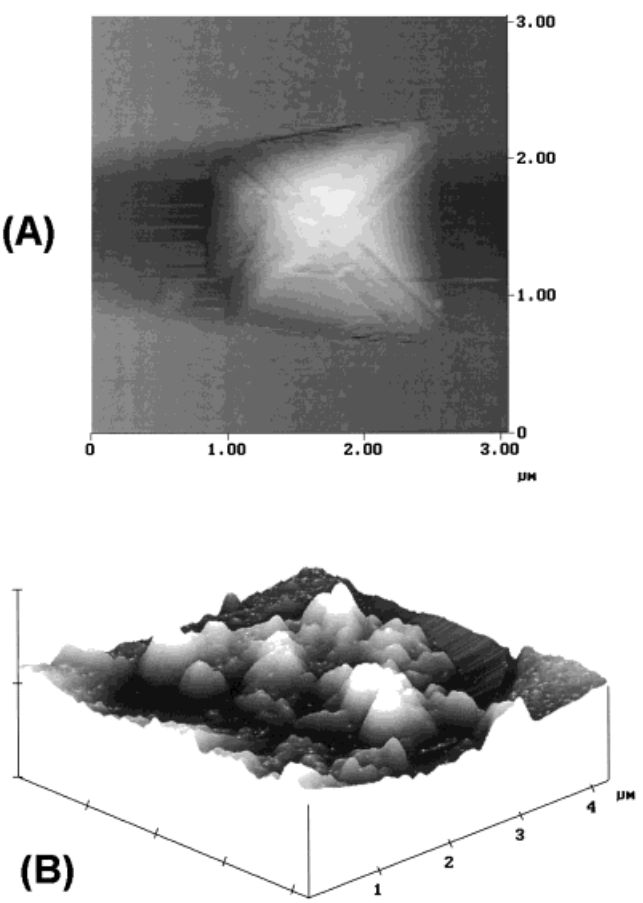

Fig. 3. AFM images of the iridium surface after five deposition/stripping cycles of mercury in a perchloric acid medium with a Ag | AgCl | 3 M NaCl reference electrode showing a typical (A) single pyramidal accumulation and (B) a cluster of pyramids.

A single pyramidal accumulation was analyzed as being only Ir. This was possibly due to the size of the pyramids and the area scanned with the Auger (5 μm^2). The accumulations were drastically affected by the Auger analysis as shown by AFM images taken before and after the analysis (Fig. 5). The mean roughness of the iridium surface increased from 0.125 to 0.182 nm and the accumulation appeared different although the shape was relatively constant. The dimensions of both the large and the small accumulation changed after Auger analysis was performed (Table 1). The decrease in size of the accumulations was due to the electron beam interacting with the pyramidal accumulation. As discussed below, this interaction was not observed with the cluster accumulations and occurred with all pyramidal accumulations.

Since elemental analysis of a single pyramid was not informative about the accumulations, Auger analysis of a cluster was performed. The accumulations were ana-

lyzed as mercury with a small amount of chloride. Chloride is difficult to analyze with Auger because it desorbs from the surface. Thus, the small amount of chloride was not a true indication of the actual amount present on the surface. Since all the liquid mercury was vaporized, we can reasonably conclude that the accumulations on the Ir-UME surface are some sort of solid mercury–chloride compound. A confirmation that no liquid mercury was left on the electrode after Auger analysis was that the AFM images were not noisy. Noisy AFM images were an indication that liquid mercury was still present on the electrode. An AFM image of the area that was analyzed with the Auger SEM (Fig. 6) showed very little change in the surface roughness and in the appearance or the dimensions of the accumulations due to the electron beam.

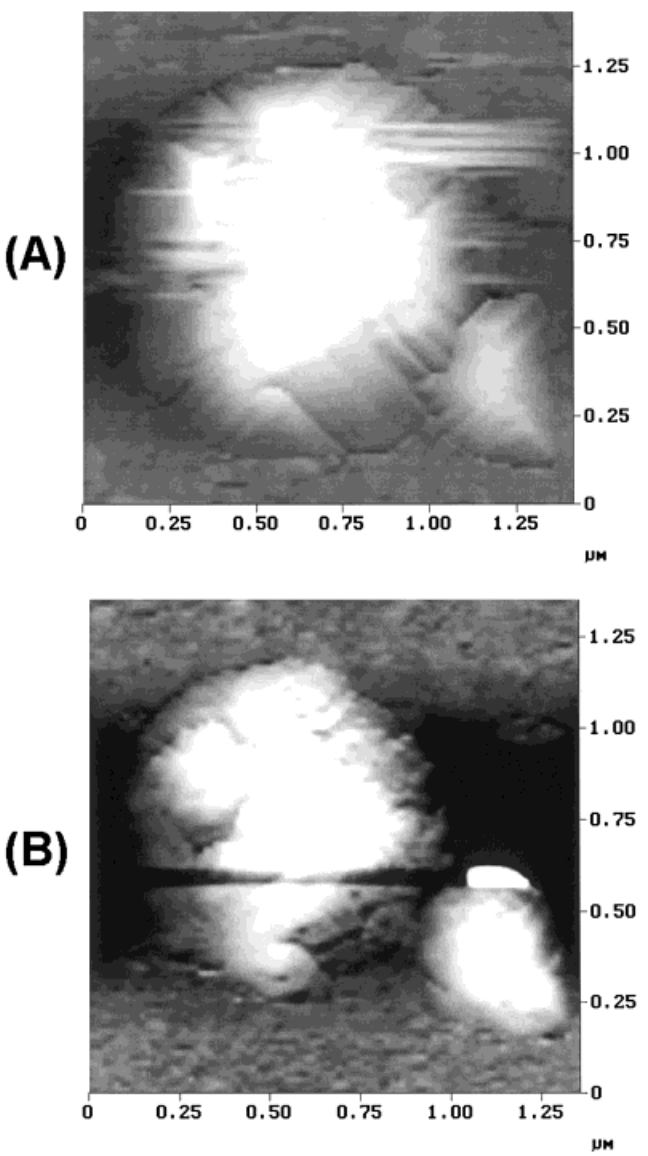

Fig. 5. AFM image of a single pyramidal accumulation (A) before and (B) after, Auger analysis.

Table 1
Dimensions of a pyramidal accumulation before and after Auger analysis was performed

	Before Auger	After Auger
Large accumulation		
Width/μm	1.26	1.01
Length/μm	1.14	0.95
Height/μm	3.17	1.8
Small accumulation		
Width/nm	454	439
Length/nm	590	577
Height/μm	1.7	1.5

3.2.2. Formation of calomel (Hg_2Cl_2)

Since mercury and chloride were both analyzed by the Auger, the accumulations were most likely either $HgCl_2$ or Hg_2Cl_2. To distinguish between these two, a classical wet chemical analysis was performed on a cluster of the pyramids. A drop of sodium hydroxide was placed on the array and the reaction was observed in-situ. Sodium hydroxide was chosen because if the accumulations were $HgCl_2$, a yellow precipitate would form and if the accumulations were Hg_2Cl_2 the solid would turn black. The latter could not be distinguished since the accumulations appeared black underneath the microscope. When sodium hydroxide was placed on the array no visible change was observed (i.e. no yellow precipitate). This along with the fact that $HgCl_2$ is soluble in water (1 g/13.5 ml) and Hg_2Cl_2 is practically insoluble in water (0.00020 g/100 ml) [22] lead to the conclusion that the accumulations were Hg_2Cl_2 (calomel). The crystalline form of calomel is tetrahedral which also corresponds to the pyramidal shapes obtained in the AFM images. Formation of Hg_2Cl_2 agrees well with the literature [23,24], which states that the anodization of mercury in the presence of chloride ions, forms calomel which precipitates on the electrode surface. Jagner et al. [25] found that a spontaneous reaction between elemental mercury on the electrode surface occurred when no potential was applied (open-circuit) in a chloride medium. Thermodynamic equi-

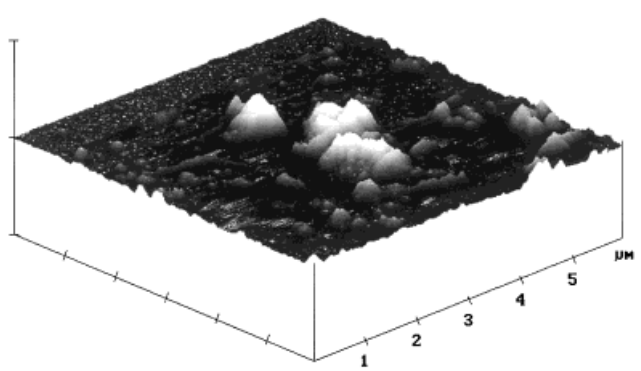

Fig. 6. A cluster of pyramidal accumulations analyzed by Auger.

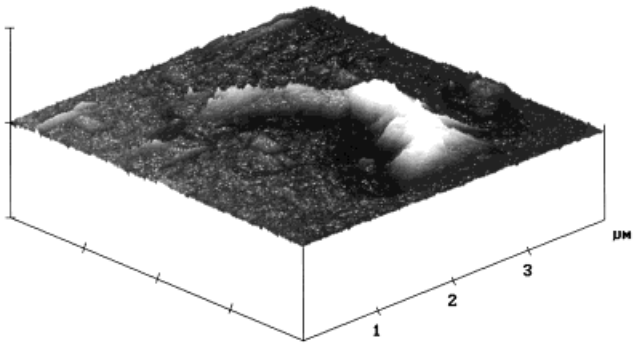

Fig. 7. Hg was deposited on an Ir-UMEA and then stored in 0.1 M NaCl for 60 s. After the Hg was stripped the surface of an Ir-UME was seen to be covered by unknown accumulations.

librium calculations showed that with chloride concentrations in the range of 0.002 to $\sim$3.5 M, formation of calomel occurred. Below this concentration (0.002 M), the excess Hg^{2+} reacted with the elemental mercury to form soluble Hg_2^{2+}. Above this concentration ($\sim$3.5 M), the mercury film remained as elemental mercury and no calomel was formed. Jagner et al concluded that Hg^{2+} must be present in the solution and that the following reaction occurred for the formation of calomel.

$$Hg + Hg^{2+} + 2Cl^- \rightarrow Hg_2Cl_2\ (s) \quad (1)$$

The formation of calomel is very rapid and occurs after the electrode is immersed in the solution for only 5 s.

Since Jagner et al. had used only a large glassy carbon electrode (3 mm), these experiments were reproduced using the Ir-UMEAs to determine whether the calomel was also formed by the above reaction. The UMEA was first coated with mercury and then placed for 60 s in a solution containing 8×10^{-3} M Hg(II) in 0.1 M NaCl and acidified to $\sim$pH 2 with HCl. The mercury was then stripped in 1 M KSCN. All the UME elements had accumulations as determined by optical microscopy. AFM images were extremely noisy due to the presence of liquid Hg on the iridium surface. Pyramidal accumulations were observed but their location was difficult to pinpoint because the AFM tip was moving liquid mercury across the surface. Another UME array was coated with mercury and stored in 0.1 M NaCl solution for 60 s. After stripping some liquid Hg still appeared to remain on the UMEs, but did not appear to interfere with acquisition of reasonably good AFM images. The images, shown in Fig. 7, reveal a cluster of calomel pyramids on the surface. Although Hg(II) was not present in this solution, it is possible that a small amount could have been accidentally transferred since the electrode was cleaned only by dipping in water before being placed in the chloride solution. The UME array was only lightly rinsed with water since more rigorous action might damage the mercury coating. If Hg(II) ions were a contaminant, then calomel formation would occur and interfere with the detection of analytes, provided that chloride ions are present in the solution.

3.2.3. Contamination of the mercury deposition solution

Since the plating and stripping solutions did not initially contain any Cl^-, the solutions must have eventually been contaminated from the components. Two obvious sources are the reference electrode and the perchloric acid solution. The Ag | AgCl | 3 M NaCl, reference electrode certainly leaked some Cl^- from its junction frit. The concentration of chloride ions entering the solution will depend on; (i) the length of time that the reference electrode is in the solution and; (ii) the age of the reference electrode, or more importantly, the condition of the frit. The same new reference electrode was used for these studies in order to minimize the latter problem.

Perchloric acid at a concentration of $\sim$0.1 M is the most widely used electrolyte for deposition of mercury films from Hg(II) solutions. There are no data in the literature in reference to the stability or dissociation of perchloric acid to give Cl^-. According to the manufacturer supplied analysis, the perchloric acid used in these studies (Fisher, Ultratrace) contained <10 ppm of Cl^-. Since no accumulations appeared during the first three mercury deposition and stripping cycles, the trace amounts of Cl^- in the perchloric acid were evidently not enough for formation of calomel. Further studies though showed that perchloric acid would dissociate over time, increasing the concentration of Cl^- in solution. A 0.1 M perchloric acid solution was tested daily for 10 days by taking a 20 ml aliquot and placing a piece of aluminum foil in it. Aluminum foil was chosen because it reacts in an acidic chloride medium and the reaction is easily observed because the foil dissolves and the solution becomes gray. The aluminum foil reacted when the solution was 2 days old. The chloride concentration was estimated to be $\sim$100 μM. Although this alone was not enough for calomel formation to occur, the combination of all three chloride sources: (i) the reference electrode leakage, (ii) the trace amount of chloride present in perchloric acid, and (iii) the decay of perchloric acid; would be enough for the formation of calomel. Thus, the Cl^- concentration depends mainly on the amount of leakage from the reference electrode and the age of the perchloric solution.

3.3. Electrodeposition of Hg in nitric acid media with a polyurethane solid state reference electrode

Jagner et al. [25] have recommended that the Cl^- concentration in the mercury plating solution be greater than 3.5 M in order to avoid the formation of calomel on the electrode surface. Electrodeposition of mercury

from a solution containing 8×10^{-3} M Hg(II), 0.1 M $HClO_4$ and 4.0 M NaCl resulted in failure of the UME array by degradation of the Al traces and insulating Si_3N_4 coating [26].

Calomel formation could be prevented only by totally eliminating Cl^- from the solution and the reference electrode. This was accomplished by changing the mercury deposition solution to contain 8×10^{-3} M Hg(II) in 0.1 M HNO_3 and a replacing the Ag | AgCl | 3 M NaCl reference electrode with a PU-SSRE [21]. After each cycle of deposition and stripping, the UME array was observed with an optical microscope. After eight cycles, small black spots (< 1 μm dia.) appeared on some of the iridium UME surfaces. However, even after ten cycles no pyramidal accumulations were observed. The only noticeable change was a slight increase in mean surface roughness (0.076 nm) as shown in Fig. 8. This increase however (vide infra) did not affect the Hg electrodeposition efficiency of the UME array. This increased roughness of the iridium UME surfaces could be due to partial oxidation of the iridium during the stripping of the mercury. This is in contrast to a much larger increase in the roughness (0.124 nm) when coating the array in a perchloric medium even only once. Some liquid mercury was still found to be present on the electrode surface, indicating that the mercury was not 100% stripped off.

Jagner et al. [25] suggested that at chloride concentration below 0.002 M, the mercury film dissolved due to the formation of soluble Hg_2^{2+}. However, no indication of the mercury completely dissolving was observed in our experiments, even when totally eliminating chloride from the mercury deposition solution.

3.4. Cross section analysis

A more detailed view of the changes in roughness of the UME iridium surface was obtained by performing a cross section surface analysis (i) prior to use, (ii) after the formation of a single pyramidal structure, (iii) with a cluster of pyramidal structures, and (iv) after deposition in nitric acid media. The results are shown in Fig. 9. Before any electrochemical use, the iridium surface appeared flat with no deformities (Fig. 9A). An almost triangular irregularity was observed after a single pyramidal accumulation on the iridium (Fig. 9B). Also, there was a small dip before the accumulation, which was due to the tip dragging on the top of the accumulation. The section analysis of the cluster covered UME (Fig. 9C) showed that they are formed by several individual pyramidal accumulations overlapping with each other. Finally, the UME iridium surface, after ten consecutive deposition/stripping cycles of mercury in the nitric media, showed only a slight increase in surface roughness and no pyramidal accumulations (Fig. 9D), as compared to the iridium before use or with chloride contamination.

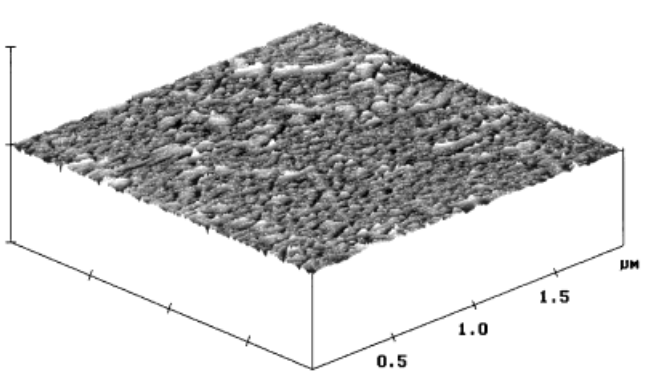

Fig. 8. The iridium UME surface after ten deposition/stripping cycles of mercury in 0.1 M HNO_3 using a PU-SSRE reference.

3.5. Efficiency of mercury deposition

The reduction (Q_{red}) and oxidation (Q_{ox}) charges were monitored for the deposition and stripping of mercury. In theory the ratio of Q_{ox}/Q_{red} should be 1 (100% efficiency), but experimentally, the percent efficiency never exceeded 41% in the perchloric acid medium and 75% in the nitric acid medium. In the perchloric medium, the average percent efficiency for the five mercury depositions was $13.9 \pm 15.7\%$. To confirm these values the experiment was performed twice with different Ir-UMEAs. The results are shown in Table 2. The efficiency was very low in the perchloric acid medium for both arrays ranging from 0.7 to 41.1%. The low efficiency can be attributed to the formation of calomel, which partially covers the mercury surface. After the mercury film has been formed on the iridium electrode, some of the liquid mercury reacts to form calomel thus decreasing the amount of mercury that will be oxidized in the stripping step. Consequently, calomel formation decreases the oxidation current and thus the efficiency. Thus, there is a direct correlation between the formation of the calomel on the iridium surface and the deteriorating performance of the UME array.

Five chronoamperometric reduction curves for deposition of Hg(II) on the UMEA, at -0.4V in a 8×10^{-3} M Hg(II) + 0.1 M $HClO_4$ solution, with a Ag | AgCl | 3 M NaCl reference electrode, are shown in Fig. 10A. The respective stripping curves for the oxidation of the deposited Hg in 1 M KSCN using a potential scanned from -0.3 to 0.3 V at 20 mV s^{-1}, are shown in Fig. 10B. The reduction curves are not very reproducible and are significantly noisy, indicative of changes in surface morphology and irregularities during the deposition. For oxidation of the mercury the currents were very irreproducible varying from 1.23 to 31.67 μA. Thus, the use of a perchloric acid medium and a Ag | AgCl | 3 M NaCl reference electrode do not appear to be conducive to depositing mercury cleanly.

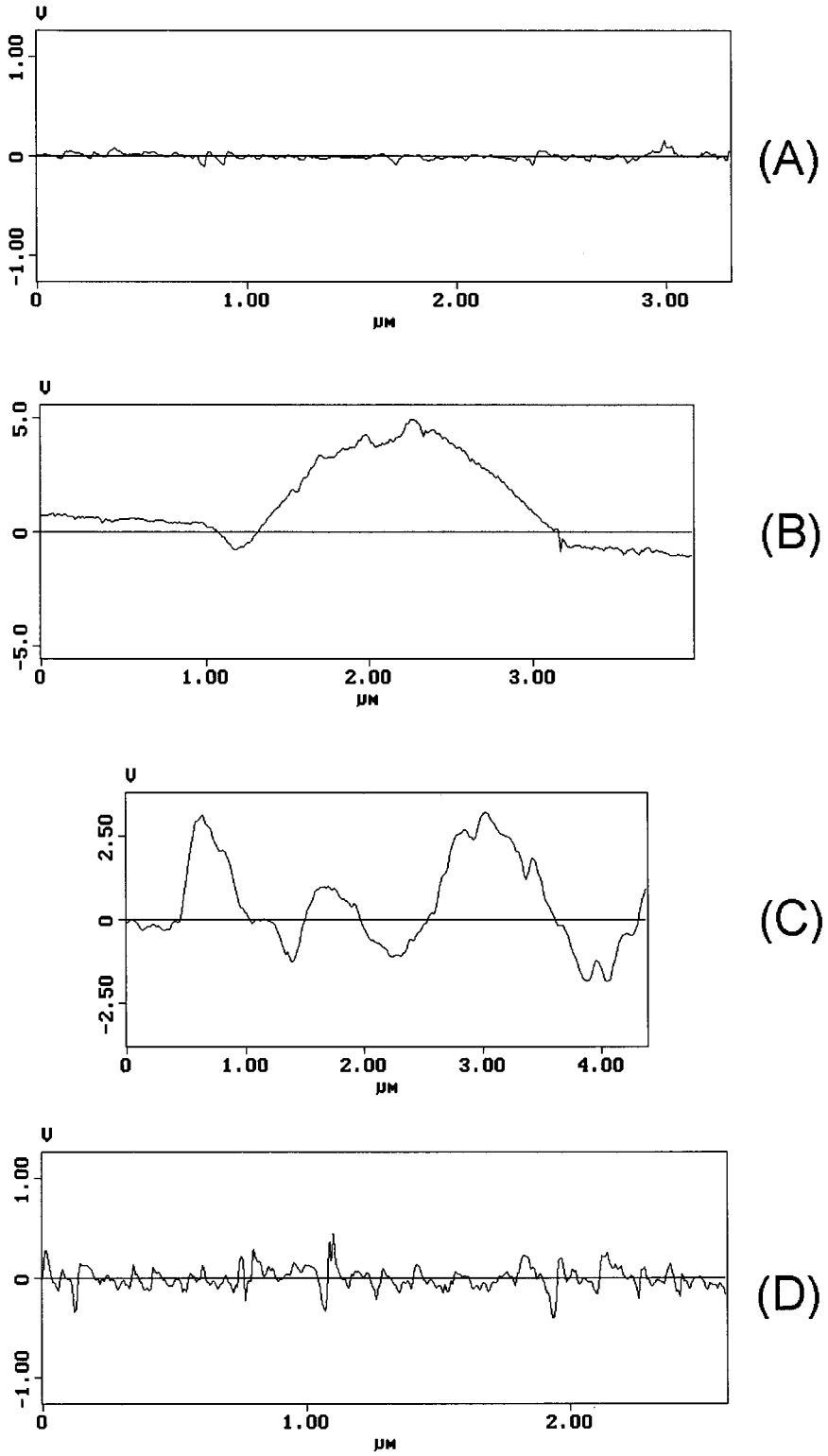

Fig. 9. Cross section AFM height analysis of an iridium UME surface (A) prior to use, (B) of a single pyramidal accumulation, (C) a cluster of pyramids and (D) an array coated ten times with mercury in a nitric acid medium with a PU-SSRE.

The efficiency and quality of the mercury deposition and stripping was greatly increased by using a nitric acid medium and a PU-SSRE (Table 3). After ten cycles the average efficiency was $67.2 \pm 4.7\%$. However, the best value, 74.8%, was obtained for the last cycle. The oxidation charge is greater since calomel is no longer being formed on the iridium UME surfaces. Efficiencies approaching 100% would not be expected

Table 2
Reduction and oxidation charge and percent efficiency for five consecutive deposition/stripping cycles of Hg in 0.1 M $HClO_4$ with a Ag | AgCl | 3 M NaCl reference electrode with two different Ir-UMEAs

No. of Hg platings	Q_{red}/μC	Q_{ox}/μC	Eff (Q_{ox}/Q_{red})/%
(A)			
1	483.2	52.97	11.0
2	481.9	198.2	41.1
3	481.6	30.35	6.30
4	482.7	4.426	0.917
5	481.6	48.14	10.0
Average			13.9 ± 15.7
(B)			
1	480.4	3.362	0.7
2	483.3	32.80	6.79
3	481.9	13.97	2.90
4	481.5	104.9	25.5
5	481.7	103.62	21.5
Average			11.5 ± 11.3

since several other factors also prevent this from happening. These include: (i) that all of the liquid Hg is not being stripped off during the oxidation step. This was confirmed by the AFM and Auger results; (ii) the Hg is chemically oxidized by traces of O_2 remaining in the solution, and (iii) the contribution of capacitive currents to the deposition charge (Q_{red}).

Table 3
Reduction and oxidation charge and percent efficiency for ten consecutive depositions/stripping cycles of Hg in 0.1 M HNO_3 with a PU-SSRE

No. of Hg platings	Q_{red}/μC	Q_{ox}/μC	Eff (Q_{ox}/Q_{red})/%
1	480.9	288.1	59.9
2	481.3	331.6	68.9
3	507.2	334.9	66.0
4	484.8	295.9	61.0
5	512.0	339.3	66.3
6	508.5	351.8	69.2
7	494.3	331.0	67.0
8	482.5	314.2	65.1
9	478.1	351.5	73.5
10	480.6	359.3	74.8
Average			67.2 ± 4.7

The reduction and oxidation curves for ten consecutive depositions of mercury in nitric acid media are shown in Fig. 11A and B. These depositions of mercury gave reproducible results with little noise as compared to mercury deposited in a perchloric acid medium. The stripping of mercury was also more reproducible in a

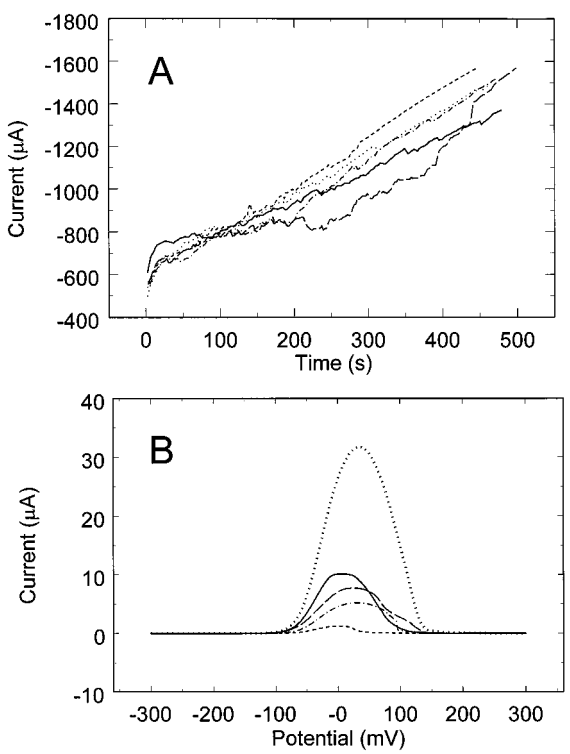

Fig. 10. Results for six Hg deposition/oxidation cycles obtained at an Ir-UMEA for (A) deposition of mercury at −0.4 V in 8×10^{-3} M Hg(II) and 0.1 M $HClO_4$ with a Ag | AgCl | 3 M NaCl reference electrode, (B) oxidation of mercury in 1 M KSCN with the potential scanned from −0.3 to 0.3 V at 20 mV s^{-1}. (1st cycle —, 5th cycle – – –).

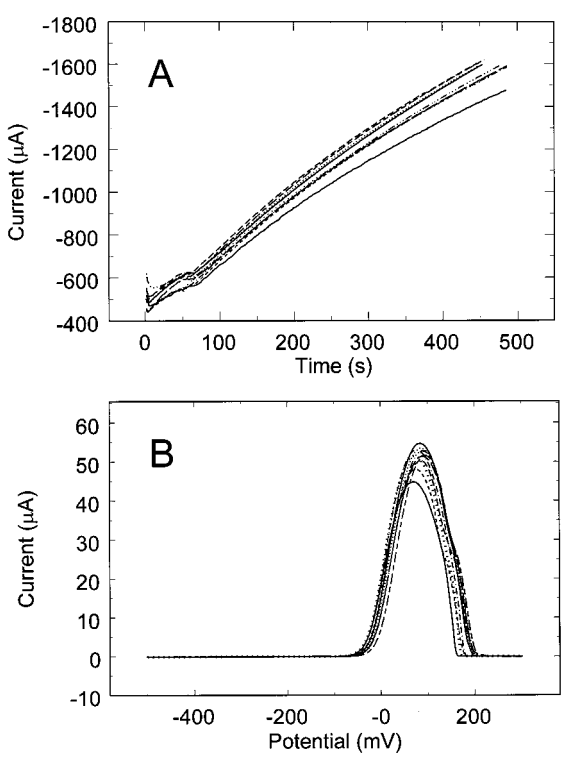

Fig. 11. Results for ten Hg deposition/oxidation cycles obtained at an Ir-UMEA for (A) deposition of Hg at −0.4 V in 8×10^{-3} M Hg(II) and 0.1 M HNO_3 with a PU-SSRE, (B) oxidation of mercury in 1 M KSCN with the potential scanned from −0.3 to 0.3 V at 20 mV s^{-1}. (1st cycle —, 9th cycle-- -)

nitric medium with peak currents varying from 45.07 to 54.61 μA. Thus, a nitric acid medium with the use of a PU-SSRE, which has no chloride leakage, was found to be an excellent method for the electrodeposition of mercury.

4. Conclusion

Eliminating chloride contamination from the mercury plating solution increased the performance and lifetime of the Ir-UMEA. Chloride contamination led to the formation of a calomel film on the electrode surface which limited the lifetime of the array to only five Hg deposition/stripping cycles. The formation of calomel also prevented a hemispherical mercury UME from forming on the iridium surface. AFM images revealed that the calomel deposits were pyramidal in shape, tended to cluster together, and increased with the number of times mercury was plated on the UME surface. Auger analysis was used to identify the accumulations but the surface was destroyed because of interactions with the electron beam. Using a nitric acid medium and a PU-SSRE appears to prolong the UMEA's lifetime with no visible surface affects. If perchloric acid must be used as the medium for electrodeposition of mercury, the solution should be freshly prepared. In addition, any contamination of the solution from leakage of the chloride containing reference electrode must be eliminated.

Acknowledgements

This work was supported in part by grants from the U.S. Environmental Protection through the Northeast Hazardous Substance Research Center at NJIT, and the National Science Foundation (CHE-9256871). The authors would like to thank the Microsystems Technology Laboratory at MIT for the microfabrication, and the Center for Materials Science and Engineering at MIT and particularly Elisabeth Shaw for her help in obtaining the Auger SEM data. We also thank Rosemary Feeney and Christine Jaworek for their valuable assistance.

References

[1] G. Sreenivas, S.S. Ang, I. Fritsch, W.D. Brown, G.A. Gerhardt, D.J. Woodward, Anal. Chem. 68 (1996) 1858.
[2] H. Sangodkar, S. Sukeerthi, R.S. Srinivasa, R. Lal, A.Q. Contractor, Anal. Chem. 68 (1996) 779.
[3] J. Wang, Q. Chem, Anal. Chem. 66 (1996) 1007.
[4] R. Hintsche, M. Paeschke, U. Wollenberger, U. Schakenberg, B. Wagner, T. Lisec, Biosens. Bioelectr. 9 (1994) 697.
[5] Q. Chen, J. Wang, G. Rayson, B. Tian, Y. Lin, Anal. Chem. 65 (1993) 251.
[6] S.P. Kounaves, W. Deng, P.R. Hallock, G.T.A. Kovacs, C.W. Storment, Anal. Chem. 66 (1994) 418.
[7] G.T. Kovacs, C.W. Storment, S.P. Kounaves, Sensors and Actuators B 23 (1995) 41.
[8] J. Herdan, R. Feeney, S.P. Kounaves, A.F. Flannery, C.W. Storment, G.T.A. Kovacs, R.B. Darling, Environ. Sci. Technol. 32 (1998) 131.
[9] C. Belmont, M.-L. Tercier, J. Buffle, G.C. Fiazccabrino, M. Koudelka-Hep, Anal. Chim. Acta 329 (1996) 203.
[10] A. Uhlig, U. Schnakenberg, R. Hintsch, Electroanalysis 9 (1997) 125.
[11] M. Paeschke, F. Dietrich, A. Uhlig, R. Hintshe, Electroanalysis 8 (1996) 891.
[12] A. Uhlig, M. Paeschke, U. Schnakenberg, R. Hintsche, H.-J. Diederich, F. Scholz, Sensors and Actuators B 24–25 (1995) 899.
[13] P.R. Fielden, T. McCreedy, Anal. Chim. Acta 273 (1993) 111.
[14] G. Binnig, C.F. Quate, Ch. Gerber, Phys. Rev. Lett. 56 (1986) 930.
[15] S.P. Kounaves, J. Buffle, J. Electroanal. Chem. 239 (1988) 113.
[16] S.P. Kounaves, W. Deng, Anal. Chem. 65 (1993) 375.
[17] M.-L. Tercier, N. Parthasarathy, J. Buffle, Electroanalysis 7 (1995) 55.
[18] S.P. Kounaves, J. Buffle, J. Electrochem. Soc. 133 (1996) 2495.
[19] C. Guminski, Z. Galus, in: C. Hirayama, C. Guminski, Z. Galus (Eds.), Solubility Data Series-Metals in Mercury, vol. 25, Pergamon Press, Oxford, 1986.
[20] R. Feeney, J. Herdan, M.A. Nolan, S.H. Tan, V.V. Tarasov, S.P. Kounaves, Electroanalysis, 10, 1998, p. 89.
[21] M.A. Nolan, S.H. Tan, S.P. Kounaves, Anal. Chem., 69, 1997, p. 1244.
[22] S. Budavari (Ed.), The Merck Index, 11th ed., Merck & Co., New Jersey, 1989.
[23] Z. Stojek, J. Osteryoung, Anal. Chem. 60 (1997) 131.
[24] M. Antonietta Baldo, S. Daniele, G.A. Mazzocchin, Anal. Chim. Acta 340 (1997) 77.
[25] D. Jagner, E. Sahlin, L. Renman, Anal. Chem. 68 (1996) 1616.
[26] M.A. Nolan, S.P. Kounaves, Sensors and Actuators B, (in press).